ELSEVIER

Computers and Electronics in Agriculture
34 (2002) 223–235

Computers and electronics in agriculture

www.elsevier.com/locate/compag

Modeling of air inlets in CFD prediction of airflow in ventilated animal houses

B. Bjerg [a,*], K. Svidt [b], G. Zhang [c], S. Morsing [c], J.O. Johnsen [c]

[a] *Royal Veterinary and Agricultural University, Grønnegaardsvej 8, DK-1870 Frederiksberg C, Denmark*
[b] *Aalborg University, Sohngaardsholmsvej 57, DK-9000 Aalborg, Denmark*
[c] *Danish Institute of Agriculture Science, Research Center Bygholm, P.O. Box 536, DK-8700 Horsens, Denmark*

Abstract

This study investigates different methods to model wall inlets in computational fluid dynamics (CFD) simulations of airflow in livestock rooms. The experiments were carried out in an 8.5 m long, 3 m high and 10.14 m wide test room equipped with a forced ventilation system. Four wall inlets were distributed symmetrically along an end wall 0.5 m beneath the ceiling. To obtain uniform and easily modeled boundary conditions the inlets were designed as rectangular frames with an elliptic profile in the contraction section following the ISO standard for a long-radius nozzle. Vertical and horizontal air speed profiles in the jets were measured with thermistor speed sensors at four distances from the inlets and an ultrasonic sensor was used for measurement of air velocity in the occupied zone close to the floor. CFD-simulations with the k–ε turbulence model were carried out with a number of different grid constructions. Both measurement and CFD simulations showed that two different airflow patterns occurred in the test room. In airflow pattern 1 the jets beneath the ceiling turned towards the symmetry plane of the room and above the floor the air flowed away from the symmetry plane. In air flow pattern 2 the jets turned away from the symmetry plane and above the floor the air flowed towards the symmetry plane. The findings in this study indicate that assuming two dimensional (2-D) inlet conditions might be a useful way to simplify inlet boundary conditions and grid constructions for prediction of air flow in the occupied zone of livestock rooms with many wall inlets. However, more work must be done to evaluate this statement in other arrangements, including changed orientation and loca-

* Corresponding author.
E-mail address: bb@kvl.dk (B. Bjerg).

PII: S0168-1699(01)00189-2

tions of inlets, unattached jets and non-isothermal conditions.

Keywords: Numerical simulation; CFD; Airflow; Inlets; Ventilation; Test room

1. Introduction

Control of airflow, temperature distribution and contaminants are essential to ensure optimal production conditions and healthy working environments in animal houses. Computational fluid dynamics (CFD) has great potential to predict these parameters, but successful use of the technique requires knowledge of suitable methods to handle boundary conditions and grid distributions in the airspace.

A general introduction to the application of CFD in room ventilation is given by Awbi (1989). This investigation focuses on boundary conditions for inlets and grid distributions in a room with a number of wall inlets located in a row at some distance from the ceiling, which is a widely used arrangement in ventilation systems in animal houses. Previous studies on CFD methods to predict airflow in animal houses have usually been based on enclosures with only one inlet. A slot inlet immediately beneath the ceiling have been used in several investigations e.g. Bjerg et al. (1999, 2000a), Hoff et al. (1992). Harral and Boon (1997) compared CFD simulation with detailed air velocity measurements in an experimental section of a typical mechanical ventilated livestock building with an air intake under the ridge. The air was directed into both sides of the experimental section but possible interaction between the air entering the two sides of the room was neglected in the simulations by calculating the air flow in one side of the section only. Murikami and Kato (1989) used CFD and model scale experiments to study airflow in rectangular rooms with one, four or nine quadratic inlets located in the ceiling. The agreement between the CFD calculations and the experiments was rather close but it is difficult to relate the investigation to typical arrangements in livestock building where the location, shape, magnitude and direction of the inlets are different. Bjerg et al. (2000b) compared methods to model a single prefabricated wall inlet and obtained good results with a geometrical model of the inlet combined with hexagonal grid oriented in the inlet direction.

In practical husbandry the inlets are often so numerous that it becomes very complicated and time consuming to model each inlet in detail and, therefore, the purpose of this investigation was to develop less complicated methods to model a number of inlets.

2. Methods

2.1. Test room

The investigation was carried out in an 8.5 m long, 3 m high and 10.14 m wide test room equipped with a forced ventilation system (see Fig. 1).

Four wall inlets were distributed symmetrically along an end wall. The center to center distance between inlets was 2.5 m. To obtain uniform and easily modeled boundary conditions the inlets were designed as rectangular frames with an elliptic profile in the contraction section following the ISO standard for a long-radius nozzle (ISO 5167, 1991; see Fig. 2). The openings were 0.525 m wide, 0.05 m high with a pitch angle 20° upward and centered 0.49 m beneath the ceiling. The airflow rate was 0.4 m^3/s at a pressure difference of 10 Pa.

2.2. Measurements

A multi-channel thermistor based omnidirectional air speed sensor system and an ultrasonic three-dimensional (3-D) velocity sensor (Windmaster, Gill instruments, England) were used for air speed and velocity measurements. The airspeed sensor system was developed at the Danish Institute of Agriculture Sciences, Research Center Bygholm and the accuracy of the sensors were better than 2% in the range from 0.3 to 10 m/s (Zhang et al., 1996). Due to their ability to measure in distinct points themistor sensors were preferred in the measurement of the jets from the four inlets. The accuracy of the ultrasonic sensor was 1.5% with a resolution of 0.01

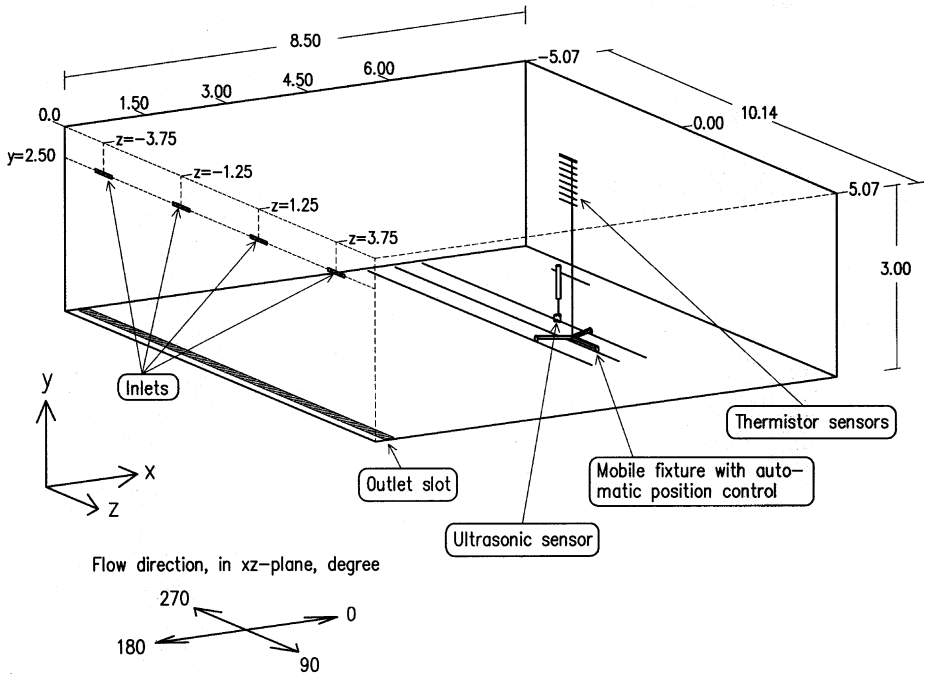

Fig. 1. Geometry of test room, coordinate system and air speed and velocity measuring equipment (dimensions are in m).

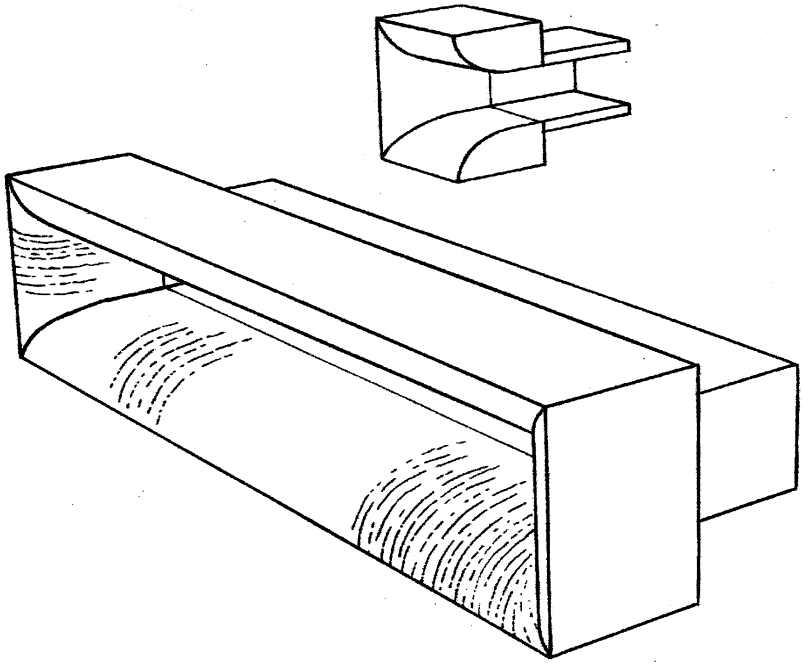

Fig. 2. Inlet designed as a rectangular frame with an elliptic profile in the contraction section following the ISO standard for a long-radius nozzle.

m/s and an offset of 0.01 m/s. Nine thermistor sensors and the ultrasonic sensor were placed on a mobile fixture with automatic position control as shown in Fig. 1. The fixture was moved on a rail oriented in the z-direction and could automatically move within about 4 m. The entire room width was covered by moving the rail. Measurements were conducted at four distances from the inlet wall $x = 1.5$, 3.0, 4.5, and 6.0 m. At $x = 1.5$, 3.0 and 4.5 m, the measurements in the z-direction were controlled from $z = -4.0$ m to $z = 4$ m with each step of 0.125 m. At $x = 6.0$ m, the measurement positions in the z-direction were controlled from $z = -4.5$ m to $z = 4.5$ m with step of 0.25 m. Measuring time at each location was 20 min and the frequency of ultrasonic sensor was one measurement per second. The positions of the velocity sensors are shown in Table 1.

2.3. CFD-simulation

Airflow was predicted by the commercial code Fluent 5 (Fluent Inc) and the k–ε turbulence model (Launder and Spalding, 1974). The constants in the k–ε turbulence model were set in accordance with the recommendations of Launder and Spalding (1974). The boundary conditions used were velocity inlet, pressure outlet

and wall functions at all surfaces. Inlet velocity was assumed to be equally distributed over the inlet areas (0.105 m^2) and determined from the measured airflow rate (0.4 m^3/s) to be 3.81 m/s. Five methods to model the inlets were investigated. A geometrical model of the four inlets, oriented and located as in the measurement, was called model A which was used as a reference case for comparing with the less complicated and easier constructed models B–E (Fig. 3). In model B the number of inlets was reduced to two, twice as wide openings. In model C we used only one opening four times as wide. In model D the opening area was distributed in a slot in the entire room width centered in the same room height as in the measurements. A corresponding slot located immediately beneath the ceiling was used in model E.

Hexagonal grids were used in all models. Close to the inlet the grid was oriented in the inlet direction in model A–D. Fig. 4 shows the cell distribution on the surfaces and on a cross section in model A. The number of cells was 85 016 in model A, declining to 43 146 in model E (see Fig. 3). Two additional simulations in model A with 21 624 and 168 680 cells, respectively, were made to investigate the convergence of the grid. The change in grid resolution was distributed equally to the entire air volume. In general the simulations were carried out with steady state conditions but to identify possible time dependency in the simulation results a transient simulation was made in model A with 85 016 cells.

3. Results and discussion

3.1. Measurements

Fig. 5 shows measured air speed profiles beneath the ceiling. The differences in the profiles measured at $x = 3.0$ m and $x = 4.5$ m are notable. At $x = 3.0$ m the

Table 1
Location (height above floor) of velocity sensors in measurements at the four distances from inlet wall

	Distance from inlet wall (m)			
	1.50	3.00	4.50	6.00
Thermistor sensors	2.98	2.98	2.975	2.975
	2.95	2.95	2.95	2.95
	2.90	2.90	2.90	2.85
	2.85	2.85	2.80	2.75
	2.80	2.80	2.70	2.65
	2.75	2.75	2.60	2.55
	2.70	2.70	2.50	2.45
	2.65	2.65	2.40	2.35
	2.60	2.60	2.30	2.25
Ultra sonic sensor	0.30	0.30	0.30	0.30

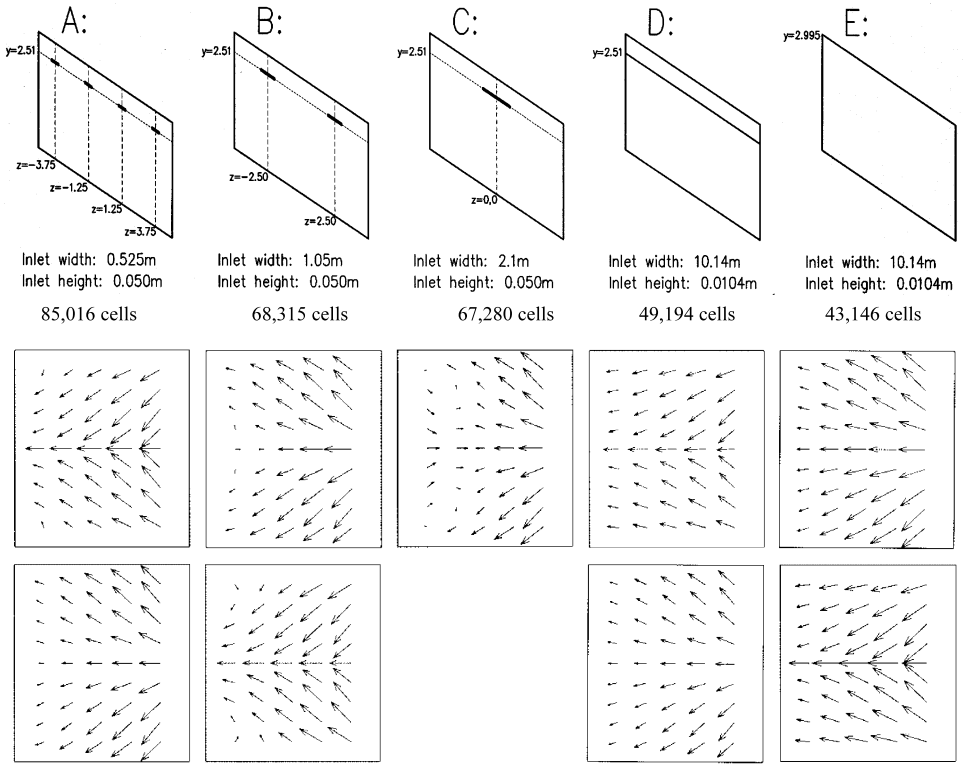

Fig. 3. Model A to E. Inlet distribution, number of cells and simulated air flow pattern 0.3 m above floor. The upper row of flow pictures shows simulation results if zero velocity initial condition was used. The lower row shows that other initial conditions could result in a different solution in model A, B, D and E. In model C the airflow pattern was impendent of the initial conditions.

highest air speed was measured in the jets from the inlets near the symmetry plane of the room (see at $z = -1.25$ and 1.25 in Fig. 5(B)), but at $x = 4.5$ m the highest air speed was measured in the jets from the inlets close to the side walls. There was a difference between the two jets close to the symmetry plane. At $x = 3.0$ m the highest air speed was measured in the jet from the inlet located at $z = -1.25$ m, but at $x = 4.5$ m the airspeed was higher in the jet from the inlet located at $z = 1.25$ m. Furthermore, in the measurements at $x = 3.0$ m all four jets turned towards the symmetry plane of the room, and at $x = 4.5$ m the jets from all 4 inlets turned away from the symmetry plane of the room. At $x = 6.0$ m the jet from the inlet at $z = -3.75$ m turned towards the symmetry plane and the three other jets turned away from the symmetry plane. All the above mentioned observations indicate that the general air flow pattern may have changed during the measurement.

Fig. 6 shows the horizontal values of the ultrasonic velocity sensor measurements 0.3 m above the floor. Comparison of Figs. 5 and 6 indicates that two types of airflow pattern were established apparent during the measurement:

Pattern 1: beneath the ceiling the jets turn towards the symmetry plane and above the floor the air flows away from the symmetry plane, which occurs at $x = 3.0$ m and $x = 6$ m for $z <= -2.0$ m.

Pattern 2: beneath the ceiling the jets turn away from the symmetry plane and above the floor the air flows towards the symmetry plane, which occurs at $x = 4.5$ m and $x = 6$ m for $z <= -1.50$ m.

The changes between the two airflow patterns only took place when the rail for the mobile sensor fixture was moved and it is likely that the location of the measuring equipments was significant in establishing what flow pattern developed when the measuring schedule was continued.

In this investigation the simultaneous movement of velocity and air speed sensors yield high measurement capacity, but using one or a number of fixed sensors to capture changes in airflow during the measurements might have improved the measurements.

3.2. Simulation

Simulated airflow patterns 0.3 m above floor are shown in Fig. 3. The upper row of air flow pictures shows the results if the initial condition for the simulation was zero velocity. The flow pattern using model A and D corresponds to flow pattern

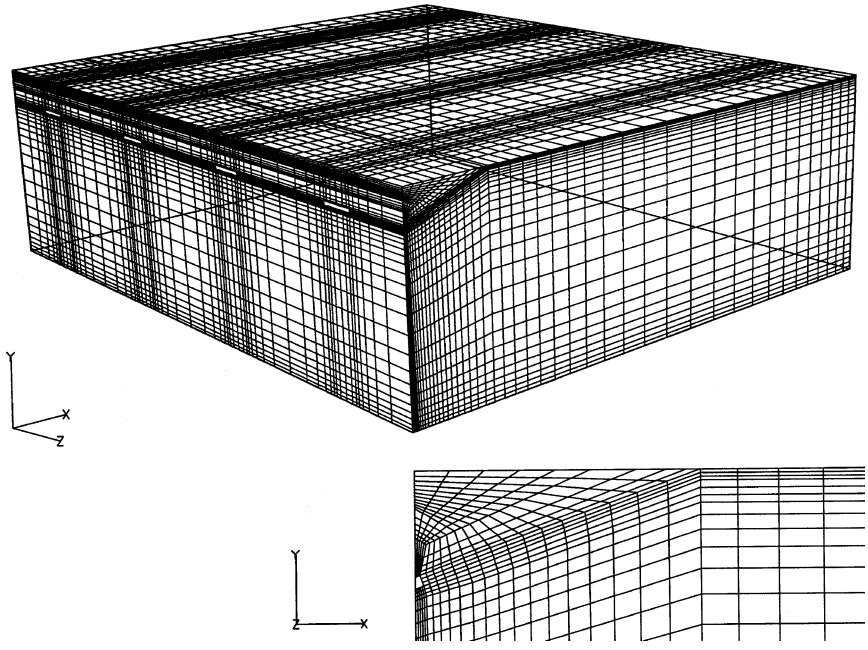

Fig. 4. Grid on surfaces and on a cross section through an inlet in model A (85 016 cells).

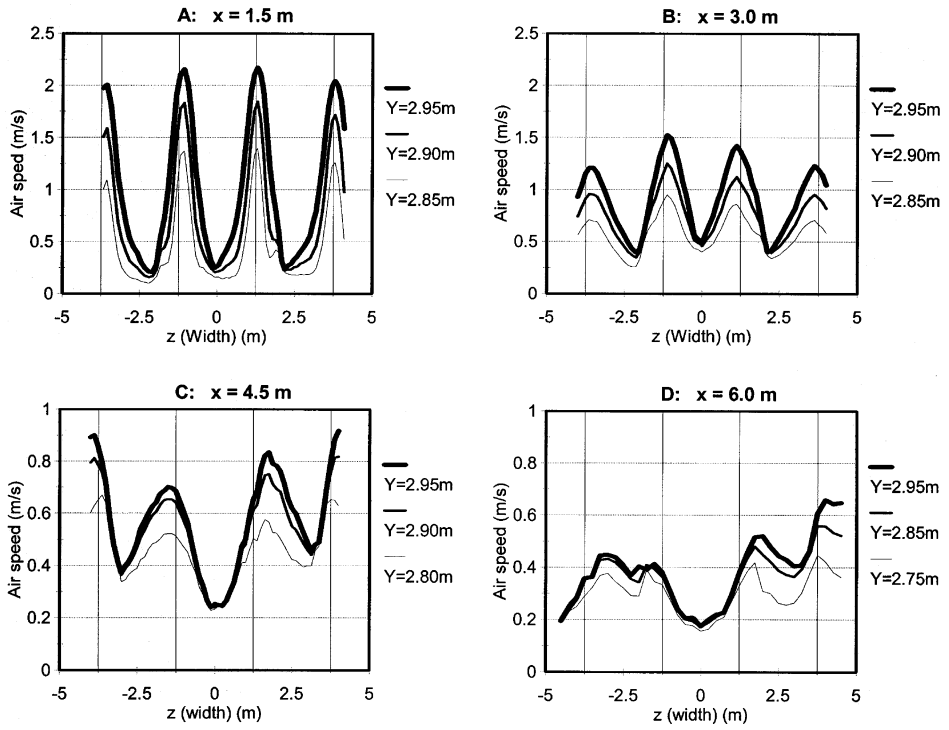

Fig. 5. Measured air speed profiles beneath the ceiling, A at $x = 1.5$ m, B at $x = 3$ m, C at $x = 4.5$ m and D at $x = 6.0$. The vertical lines show the locations of symmetrical planes of inlets.

2 (described in the measurement section) and the flow pattern using model B, C and E corresponds to pattern 1. The lower row of flow pictures in Fig. 3 shows that for model A, B, D and E it was possible to obtain a converged solution with the opposite flow pattern. These solutions were developed in two steps. Firstly, the flow pattern was established by adding a transverse velocity component (z-direction) to the inlet velocity. In model A and D the transverse velocity component was oriented in the direction of the nearest side wall, and in model B, C and E it was oriented in the direction of the symmetry plane of the room. Secondly, the traverse direction of inlet velocity was removed and only in model C the flow pattern changed.

It appears from the flow pictures in Fig. 3 that all simulated air flows were symmetrical around the symmetry plane of the room. Earlier work showed that simulations with other room dimensions resulted in asymmetrical air flow, although the boundary conditions were symmetrical (Bjerg et al., 1999).

The transient simulations carried out in model A (85 016 cells) converged to same stable solution as the steady state simulation and consequently there was no sign of time dependency in the simulation results.

Fig. 7 compares measured and simulated air velocity components 0.3 m above the floor at $x = 4.5$ m and both measuring and simulation results originate from air flow pattern 2. Fig. 8 shows the same parameters from $x = 3$ m where the results originate from air flow pattern 1.

The measured air flow was asymmetrical in both airflow patterns (e.g. at $x = 3$ m and $x = 4.5$ m). The reason for the asymmetrical airflow might be disturbances from measuring equipment or uncertainties in the presumed symmetrical boundary conditions. Since the simulated airflow was symmetrical it will not be possible to obtain an exact prediction of air velocities in the occupied zone. Figs. 7 and 8 show that the differences between the simulation results using model A, B, D and E were small and the simulated velocity in the x- and z-direction were relatively close to the measured values. All the simulations resulted in positive values of the velocity in the y-directions close to symmetry plane at $x = 4.5$ (see Fig. 7) which was not found in the measurements. The general airflow pattern was unaffected by changes in the number of cells from 21 626 to 168 680 cells in model A, but especially around the symmetry plane at $x = 3.0$ m (Fig. 8) the increase of cells resulted in increased air velocity in the x-direction. Comparison of the simulation results from

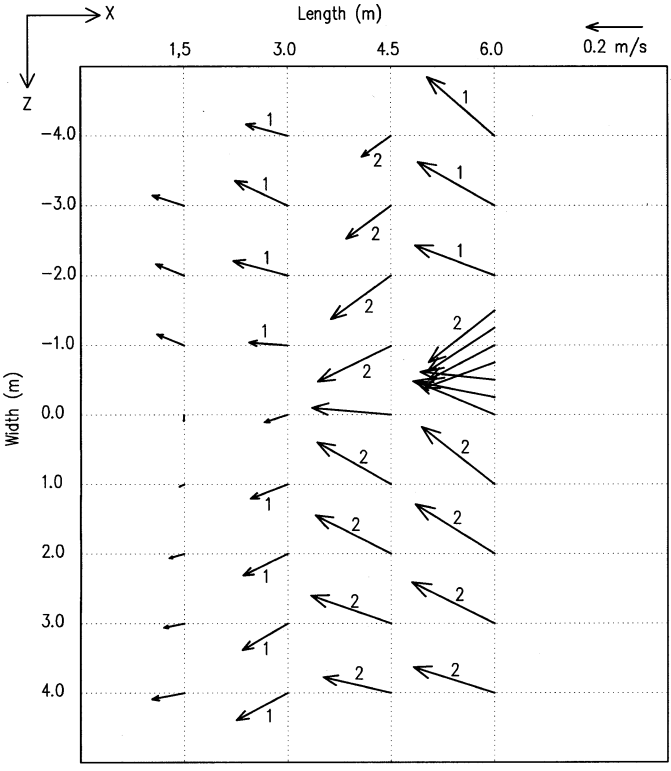

Fig. 6. Ultrasonic velocity measurements of air flow 30 cm above the floor. 1 and 2 marked mean air flow pattern 1 and 2, respectively.

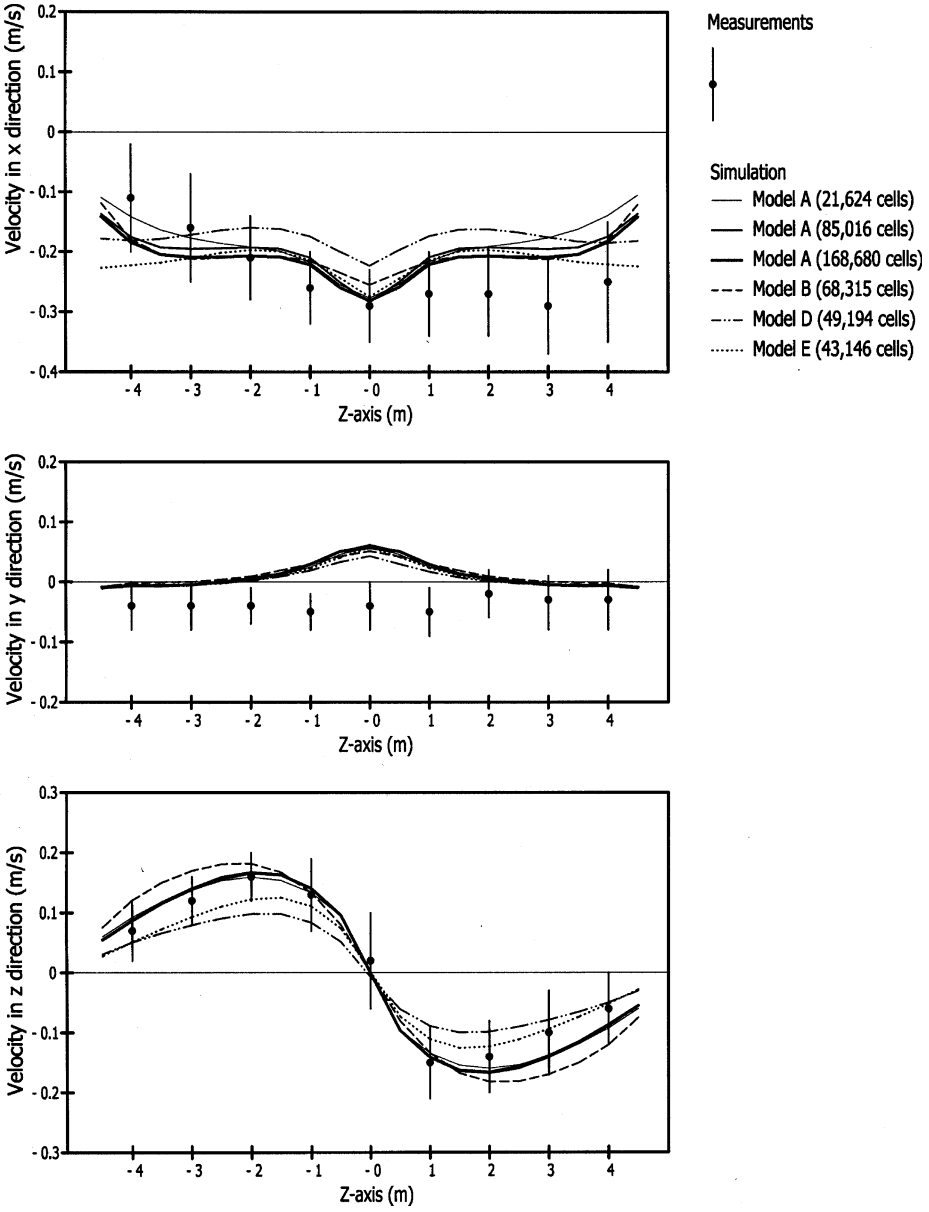

Fig. 7. Measured and simulated air velocity 0.3 m above floor at $x = 4.5$ m. The results originate from airflow pattern 2 and the markers used for measurements show mean value and standard deviation (S.D.) of 1200 scans of 1 s.

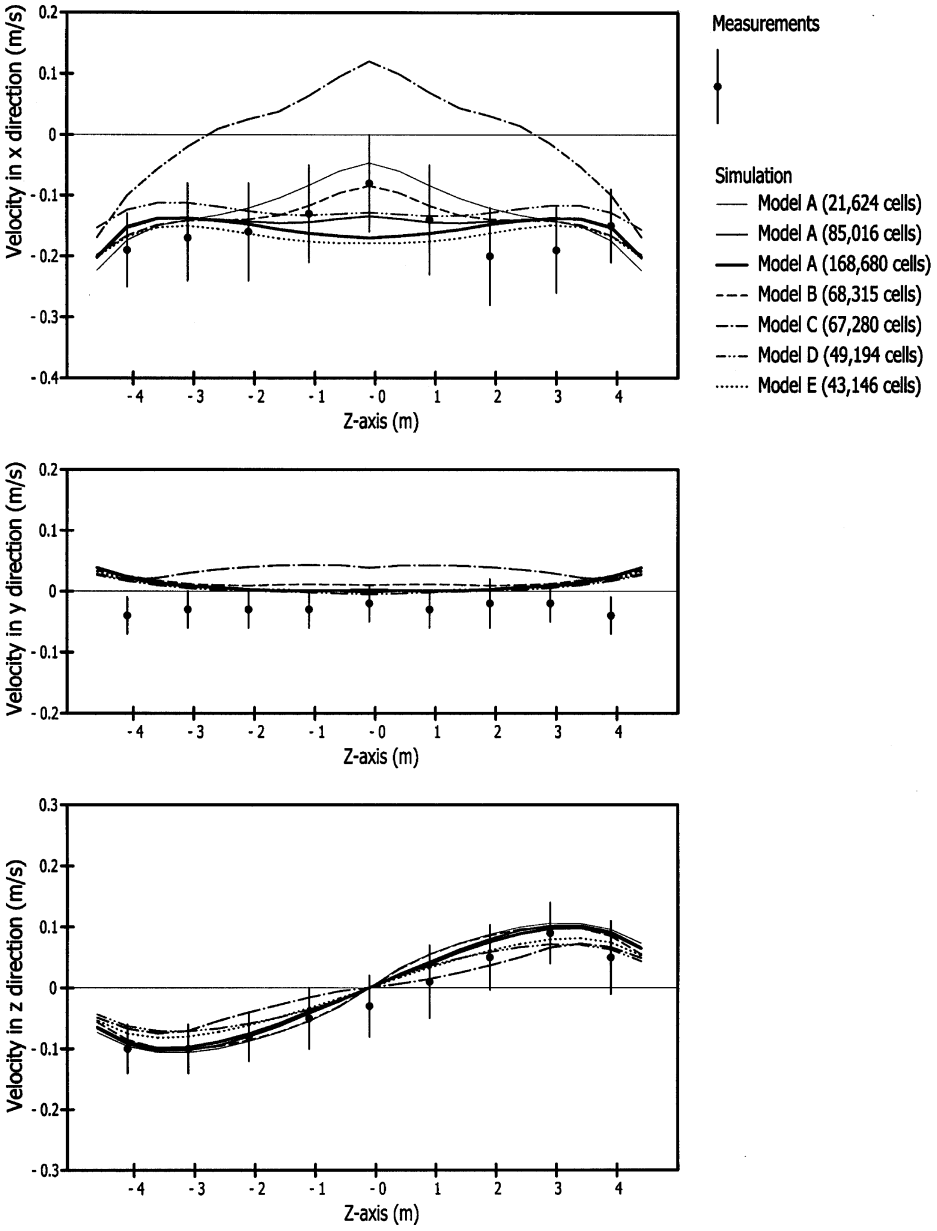

Fig. 8. Measured and simulated air velocity 0.3 m above floor at $x = 3$ m. The results originate from airflow pattern 1 and the markers used for measurements show mean value and standard deviation of 1200 scans of 1 s.

models A and B showed that the reduction of number of inlets from four to two had a very limited influence of the air flow in the occupied zone. Opposite to that the results from model C showed that the conversion of the four inlets to only one had a major influence on the air velocity in the x-direction at $x = 3$ where the simulated air flow direction was misjudged between $z = -3$ and $z = 3$ as it can be seen from Fig. 8. Air flow pattern 2 could not be established using model C and, therefore, this model is not included in Fig. 7. In model D, where the four inlets were converted to a slot in the entire room width the predicted air velocity was somewhat lower than in the result from model A—but nevertheless the prediction was relatively close to the measured values at the majority of the measuring points. The slot was located immediately beneath the ceiling in model E and consequently the simulated air speed was increased compared with model D. Figs. 7 and 8 show that the results from model E are close to the results from model A and that it is difficult to determine which of them agrees best with the measurements.

The fact that a model with two-dimensional (2-D) inlet conditions (model E) was equal to a geometric model of the four inlets (model A) in predicting the airflow in the occupied zone is remarkable, because it is much easier to generate a model with 2-D inlet condition. This result indicates that assuming 2-D inlet condition might be a useful way to simplify inlet boundary conditions and grid constructions in prediction of air flow in the occupied zone of livestock rooms with many inlets. The present work is based on a single arrangement and it is obvious that the simple conversion from a number of inlets to a 2-D opening immediately beneath the ceiling is only suitable within a limited range of inlet locations and directions. However, it can be anticipated that investigation of arrangements with other inlet directions and locations can lead to development of a more a general guideline for this conversion.

4. Conclusions

The study showed that two different 3-D airflow patterns can appear in a test room with four inlets and both flow patterns can be generated in CFD simulations. Each flow pattern was apparently stable when it was established. In the test room it only changed when the measuring equipment was moved and transient simulation showed no time dependency in the CFD results. With the used room dimension all simulation results were symmetrical around the symmetry plane of the room. Opposite to that there were some asymmetry in the measured air flow which probably was caused by disturbance from measuring equipment or uncertainties in the presumed symmetrical boundary conditions. The problem of disturbances from the measuring equipment is potential in all studies where one or a limited number of sensors are moved manually or automatically around in the air volume and it can be recommended to add one or a number of fixed sensors to capture possible changes in airflow during the measurements. Considering that the measured asymmetry was not reproduced in the simulation there was a rather good agreement between the measured and simulated airflow in the occupied zone even when the

simulations were carried out with simplified inlet boundary conditions where the four inlets where converted to a slot in the entire room width. This result indicates that assuming 2-D inlet condition might be a useful way to simplify inlet boundary conditions and grid constructions in prediction of air flow in the occupied zone of livestock rooms with many inlets. However, more work has to be done to evaluate this result in other arrangements, including changed orientation and locations of inlets, unattached jets and non-isothermal conditions.

References

Awbi, H., 1989. Application of computational fluid dynamics in room ventilation. Building and Environment 24 (1), 73–84.

Bjerg, B., Morsing, S., Svidt, K., Zhang, G., 1999. Three-dimensional airflow in a livestock test room with two-dimensional boundary conditions. Journal of Agricultural Engineering Research 74, 267–274.

Bjerg, B., Svidt, K., Zhang, G., Morsing, S., 2000a. The effects of pen partitions and thermal pig simulators on Airflow in a livestock test room. Journal of Agricultural Engineering Research 77, 317–326.

Bjerg, B., Svidt, K., Morsing, S., Zhang, G., Johnsen, J.O., 2000b. Comparison of methods to model a wall inlet in numerical simulation of airflow in livestock rooms. Paper 00-FB-024 from AgEng 2000 Warwick, UK.

Harral, B.B., Boon, C.R., 1997. Comparison of predicted and measured air flow patterns in a mechanically ventilated livestock building without animals. Journal of Agricultural Engineering Research 66, 221–228.

Hoff, S.J., Janni, K.A., Jacobsen, L.D., 1992. Three-dimensional buoyant turbulent flows in a scaled model slot-ventilated, livestock confinement facility. Transactions of the ASAE 35 (2), 671–686.

ISO 5167, 1991. Measurement of fluid by means of pressure differential devices. -Part 1: orifice plates, Nozzle and Venturi tube inserted in circular cross-section conduits running full. International organization for Standardization, Genève, Switzerland.

Launder, B.E., Spalding, D.B., 1974. The numerical computation of turbulent flows. Computer Methods of Applied Mechanical Engineering 3, 269–289.

Murikami, S., Kato, S., 1989. Numerical and experimental study on room airflow—3-D predictions using the k-ε turbulence model. Building and Environment 24 (1), 85–97.

Zhang, G., Strøm, J., Morsing, S., 1996. Computerized multipoint temperature and velocity measurement system. Proceedings of ROOMVENT'96, Fifth International Conference on Air Distribution in Rooms, 17–19 July, Yokohama, Japan.